Proc. Natl. Acad. Sci. USA
Vol. 86, pp. 7149–7153, September 1989
Medical Sciences

Labeling monoclonal antibodies and F(ab′)$_2$ fragments with the α-particle-emitting nuclide astatine-211: Preservation of immunoreactivity and *in vivo* localizing capacity

(antibody modification/radioimmunotherapy/tumor localization/astatination)

MICHAEL R. ZALUTSKY*†‡, PRADEEP K. GARG*, HENRY S. FRIEDMAN§, AND DARELL D. BIGNER†

Departments of *Radiology, †Pathology, and §Pediatrics, Duke University Medical Center, Box 3808, Durham, NC 27710

Communicated by Alfred P. Wolf, May 30, 1989 (received for review January 2, 1989)

ABSTRACT **α-Particles such as those emitted by ^{211}At may be advantageous for radioimmunotherapy since they are radiation of high linear energy transfer, depositing high energy over a short distance. Here we describe a strategy for labeling monoclonal antibodies and F(ab′)$_2$ fragments with ^{211}At by means of the bifunctional reagent *N*-succinimidyl 3-(trimethylstannyl)benzoate. An intact antibody, 81C6, and the F(ab′)$_2$ fragment of Me1-14 (both reactive with human gliomas) were labeled with ^{211}At in high yield and with a specific activity of up to 4 mCi/mg in a time frame compatible with the 7.2-hr half-life of ^{211}At. Quantitative *in vivo* binding assays demonstrated that radioastatination was accomplished with maintenance of high specific binding and affinity. Comparison of the biodistribution of ^{211}At-labeled Me1-14 F(ab′)$_2$ to that of a nonspecific antibody fragment labeled with ^{211}At and ^{131}I in athymic mice bearing D-54 MG human glioma xenografts demonstrated selective and specific targeting of ^{211}At-labeled antibody in this human tumor model.**

From a radiobiological perspective, nuclides that emit α-particles could offer advantages for certain radiotherapeutic applications. For example, 6- to 8-MeV α-particles (1 eV = 1.602×10^{-19} J) have a range in tissue of 55–80 μm, providing the potential for matching the cellular specificity of a monoclonal antibody (mAb) and radiation with cytotoxic effects limited to only a few cell diameters. These α-particles have a linear energy transfer (LET) of maximum relative biological effectiveness about 8 times that of β- or γ-radiation (1). The cytotoxic effects of high-LET radiations are thought to be irreparable (2), presumably due to the relatively high proportion of non-rejoining DNA strand breaks that they have been observed to induce *in vitro* (3). Since the cytotoxic effects of α-particles are nearly oxygen-independent (1), eradication of hypoxic tumor-cell populations also might be possible.

Two α emitters of potential utility for labeling mAbs are ^{212}Bi and ^{211}At, which have half-lives of 61 min and 7.2 hr, respectively. ^{212}Bi-labeled mAbs have been shown to be specifically cytotoxic to tumor cells both *in vitro* (4) and *in vivo* (5). For most potential clinical applications, the longer physical half-life of ^{211}At is more compatible with the rate of mAb uptake in tumor. *In vitro* studies using astatide have documented the extreme cytotoxicity of ^{211}At (6). However, the lack of suitable methods for the radioastatination of proteins has impeded the utilization of ^{211}At-labeled mAbs for radiotherapeutic studies.

Since astatine is a halogen, it might be expected that standard protein radioiodination methods could be adapted for ^{211}At labeling. Unfortunately, proteins labeled with ^{211}At by these approaches are deastatinated rapidly both *in vitro* and *in vivo* (7, 8). In order to ensure the formation of an aryl astatide bond, a method was developed for astatinating proteins via acylation with *p*-astatobenzoic acid (9). Although this approach has markedly increased the *in vivo* stability of ^{211}At-labeled proteins, even after subsequent optimization (10) the radiochemical yield and specific activity (maximum of 1 astatine atom per 20,000 protein molecules) are inadequate to permit meaningful biological evaluation of the radiotherapeutic potential of ^{211}At-labeled mAbs.

This paper describes a method that utilizes *N*-succinimidyl 3-(trimethylstannyl)benzoate (*m*-MeATE; ATE, "alkyltin ester") for labeling mAbs with ^{211}At. An IgG2b immunoglobulin and an IgG2a F(ab′)$_2$ fragment were labeled with ^{211}At in high yield and maintained immunoreactivity and affinity after astatination. Moreover, biodistribution studies in athymic mice bearing subcutaneous tumors indicated that selective tumor uptake of ^{211}At can be achieved following administration of ^{211}At-labeled mAbs.

MATERIALS AND METHODS

mAbs. mAb 81C6 (11), an IgG2b, defines an epitope of the tumor-associated extracellular matrix glycoprotein tenascin that is present in gliomas, medulloblastomas, sarcomas, Wilms tumor, and breast carcinomas (12). mAb Me1-14 is an IgG2a reactive with tumor-associated chondroitin sulfate proteoglycan present in melanomas, gliomas, and medulloblastomas (13). RPC 5 (Bionetics Research Institute) is an IgG2a that does not bind to any known antigen. Methods for the production of F(ab′)$_2$ fragments from Me1-14 and RPC 5 have been described (14).

Labeling mAbs with ^{211}At. ^{211}At was produced on a CS-30 cyclotron using the ^{209}Bi(α, 2n)^{211}At reaction by bombarding natural bismuth metal with 28-MeV α-particles. Targets consisted of a 0.3-mm layer of bismuth melted onto a 0.3-mm-thick aluminum disk. Targets were irradiated for 1.5–2.5 hr at an α-particle beam current of 12–18 μA. ^{211}At was isolated from the target by a modification of a published procedure (15, 16). The distillation temperature was increased to 715–750°C and the distillation time decreased to 15–30 min. The ^{211}At activity was collected in two bubblers in series, each containing 0.8 ml of $CHCl_3$ chilled to −20°C.

The synthesis of *m*-MeATE and *N*-succinimidyl 3-(tri-*n*-butylstannyl)benzoate (*m*-BuATE) has been described (17, 18). *N*-succinimidyl 3-[^{211}At]astatobenzoate (NS[^{211}At]AB) was synthesized by adding 20 μl (20 μmol) of *t*-butyl hydroperoxide and 5 μmol of *m*-MeATE (or *m*-BuATE) to the $CHCl_3$ trap containing the ^{211}At activity. After a 15-min

The publication costs of this article were defrayed in part by page charge payment. This article must therefore be hereby marked "*advertisement*" in accordance with 18 U.S.C. §1734 solely to indicate this fact.

Abbreviations: mAb, monoclonal antibody; ATE, alkyltin ester; *m*-MeATE, *N*-succinimidyl 3-(trimethylstannyl)benzoate; *m*-BuATE, *N*-succinimidyl 3-(tri-*n*-butylstannyl)benzoate; NS[^{211}At]AB, *N*-succinimidyl [^{211}At]astatobenzoate; % ID/g, percent injected dose of nuclide per gram of tissue.

‡To whom reprint requests should be addressed.

Downloaded at Palestinian Territory, occupied on November 28, 2021

reaction at 25°C, the mixture was evaporated to dryness and the residue was dissolved in 50 μl of $CHCl_3$. Initially, NS[^{211}At]AB was isolated by using a silica Sep-Pak cartridge (Waters) as described (15). In later experiments, NS[^{211}At]-AB was purified by high-pressure liquid chromatography (HPLC) on an Alltech Associates silica gel column, using elution with hexane/ethyl acetate/acetic acid (70:30:0.12, vol/vol).

The NS[^{211}At]AB was tranferred to a 1-dram glass vial (1 dram ≈3.7 ml) and evaporated to dryness. Between 100 and 400 μg of either 81C6 IgG or Me1-14 F(ab′)$_2$ in 50–100 μl of 100 mM borate buffer (pH 8.5) were added and, following a 15-min incubation at 4°C, 300 μl of 200 mM glycine in borate buffer was added to terminate the reaction. The ^{211}At-labeled mAbs were isolated by Sephadex G-25 column chromatography using elution with 100 mM phosphate buffer (pH 7.4). For the paired-label biodistribution studies, RPC 5 and Me1-14 F(ab′)$_2$ fragments were labeled with ^{131}I by using HPLC-purified *N*-succinimidyl 3-[^{131}I]iodobenzoate, as described (17, 18).

Immunoreactivity Assessment. *In vitro* binding of astatinated mAbs to homogenates of antigen-positive D-54 MG human glioma tumor and antigen-negative rat liver was determined in triplicate as described (19). The present ^{211}At activity bound to liver was considered to represent nonspecific binding and was subtracted from the percent bound to D-54 MG tumor in order to calculate the specific binding percentage.

The affinity constant for ^{211}At-labeled Me1-14 F(ab′)$_2$ was determined using the antigen-positive TE-671 human medulloblastoma line (20) with antigen-negative human fibroblasts (21) used to determine nonspecific binding. Serial dilutions of ^{211}At-labeled Me1-14 F(ab′)$_2$ were added in quadruplicate to 2×10^4 cells of both lines and incubated for 3 hr at 25°C. Scatchard analyses were performed using the equilibrium binding data analysis program as modified by McPherson (22).

Biodistribution Measurements. Subcutaneous tumors from the D-54 MG human glioma cell line were passaged in BALB/c *nu/nu* athymic mice by injecting 50 μl of tumor homogenate in the right flank of each recipient animal. Biodistribution studies were initiated when the average tumor volume was about 300 mm^3.

With ^{211}At-labeled mAbs, true paired-label studies are not possible because of the lack of a suitable astatine nuclide for labeling a nonspecific control mAb. In order to determine the magnitude and specificity of ^{211}At-labeled mAb uptake by tumors, two sets of experiments were performed. In the first, mice were injected in the tail vein with ^{211}At-labeled Me1-14 F(ab′)$_2$ (5 μg, 7 μCi; 1 μCi = 37 kBq) and ^{131}I-labeled RPC 5 F(ab′)$_2$ (5 μg, 4 μCi). In the second, mice received ^{211}At-labeled RPC 5 F(ab′)$_2$ (5 μg, 8 μCi) and ^{131}I-labeled Me1-14 F(ab′)$_2$ (4 μg, 5 μCi). Mice were euthanized by halothane overdose at 3, 5, 7, 14.5, and 24 hr, approximating the times at which the injected ^{211}At had decayed to 75%, 60%, 50%, 25%, and 10% of initial levels. The biodistribution of ^{211}At-labeled Me1-14 F(ab′)$_2$ alone also was determined in mice at 16 hr. Animals were dissected, and tissues of interest were weighed and assayed for ^{211}At and ^{131}I. Counting data were corrected for crossover of ^{131}I in the ^{211}At gate and for physical decay of ^{211}At and ^{131}I. Biodistribution data were expressed as (*i*) percent injected dose of nuclide per gram of tissue (% ID/g); (*ii*) tumor/normal tissue ratio; and (*iii*) localization index, the ratio of ^{211}At-labeled Me1-14 F(ab′)$_2$ to nonspecific activity (either coadministered ^{131}I-labeled RPC 5 F(ab′)$_2$ or ^{211}At-labeled RPC 5 F(ab′)$_2$ from the second set of mice) in tumor or other tissues divided by the same ratio in blood (23).

Radiation absorbed doses in rads (cGy) for a hypothetical 100-μCi dose of ^{211}At-labeled Me1-14 or RPC 5 F(ab′)$_2$ fragments were calculated from the formula

$$D = 2.13 \sum_i n_i E_i \phi_i \times 1.44 C T_e.$$

Values for n_i, the mean number of particles per nuclear transformation, and E_i, the mean particle energy in MeV, were obtained from the ^{211}At nuclear data of Lambrecht and Mirzadeh (16). The equilibrium absorbed dose constant calculated for ^{211}At α-particles was 14.445 g·rad/μCi·hr. The error introduced by ignoring the dose contribution from x-rays, γ-rays, and Auger electrons is <1%. Because of the short range of α-particles in tissue, absorbed fractions, ϕ_i, of 1 were assumed. The mean % ID/g data from the biodistribution studies were plotted to determine the initial concentration of activity, *C*, in μCi·hr and the effective half-life (T_e) in each tissue. As a first approximation, a uniform distribution of ^{211}At in tissues was assumed.

RESULTS

Labeling mAbs with ^{211}At. Between 1.5 and 5 mCi of ^{211}At was produced following 1.5- to 2.5-hr bombardments with beam currents of 12–18 μA. After a 15- to 30-min distillation at 715–750°C, 50–60% of the ^{211}At could be isolated from the cyclotron target with >90% of the activity located in the first $CHCl_3$ trap. Initial studies comparing *m*-MeATE and *m*-BuATE as precursors for the synthesis of NS[^{211}At]AB showed 10–15% higher yields with the trimethylstannyl compound. After a 15-min reaction with *m*-MeATE, 90–95% of the ^{211}At activity was isolated as the desired product. Use of the Sep-Pak procedure provided an inadequate purification of NS[^{211}At]AB, as reflected by 25 ± 3% lower protein coupling efficiencies and decreased immunoreactivities. However, HPLC gave a good separation of NS[^{211}At]AB (retention time, 11.6 min) from *m*-MeATE (retention time, 8.6 min). After HPLC purification, NS[^{211}At]AB was reacted with 81C6 IgG2b or the F(ab′)$_2$ fragments of Me1-14 or RPC 5, and 57 ± 8% of the ^{211}At activity was coupled to the mAb after a 15-min reaction; no differences were observed among the three proteins. With initial ^{211}At activity levels of 1.5–5 mCi, mAbs have been labeled at specific activities of 0.8–4 mCi/mg.

Evaluation of Immunoreactivity. For astatinated 81C6, binding to D-54 MG human glioma and antigen-negative liver homogenates was 84.2 ± 2.5% and 12.2 ± 3.5%, respectively. The average specific binding percentage for three ^{211}At-labeled 81C6 preparations ranged from 71% to 73%. The specific binding of initial preparations of 81C6 utilizing Sep-Pak-purified NS[^{211}At]AB were ≤60%. For 10 preparations of ^{211}At-labeled Me1-14 F(ab′)$_2$ using HPLC-purified NS[^{211}At]AB, binding to D-54 tumor and rat liver was 62.7 ± 5.7% and 5.6 ± 1.8%, respectively, yielding a mean specific binding percentage of 57 ± 6%. Specific binding percentages for the F(ab′)$_2$ preparations used in tissue distribution studies were 61% for ^{211}At-labeled Me1-14, 2% for ^{131}I-labeled RPC 5, 69% for ^{131}I-labeled Me1-14, and 3% for ^{211}At-labeled RPC 5. Scatchard analysis of the binding of ^{211}At-labeled Me1-14 F(ab′)$_2$ to TE-671 medulloblastoma cells revealed an affinity constant of $(1.0 \pm 0.1) \times 10^9$ M^{-1} (correlation coefficient, 0.96) with an average of 3×10^5 mAb binding sites per cell (Fig. 1).

Antibody Biodistribution. ^{211}At-labeled Me1-14 F(ab′)$_2$ levels in D-54 MG human glioma xenografts reached 11.0 ± 2.4% ID/g by 3 hr and were >12% ID/g until 24 hr, at which time they had decreased to 8.7 ± 2.1% ID/g (Fig. 2). In contrast, levels of ^{131}I-labeled RPC 5 F(ab′)$_2$ decreased rapidly from 4.7 ± 1.2% ID/g at 3 hr to 0.76 ± 0.27% ID/g at 24 hr. Similar tumor localization was observed in the second experiment when the mAb labels were reversed. In both studies, differences in tumor uptake were statistically significant (Student's *t* test; $P < 0.01$, 3 hr; $P < 0.001$, 5–24 hr). With Me1-14 F(ab′)$_2$, no significant differences were observed in tumor localization of ^{211}At and ^{131}I until 24 hr, at which time the ^{131}I-labeled mAb exhibited higher uptake (12.8 ± 2.8% versus 8.7 ± 2.1% ID/g, $P < 0.05$).

Downloaded at Palestinian Territory, occupied on November 28, 2021

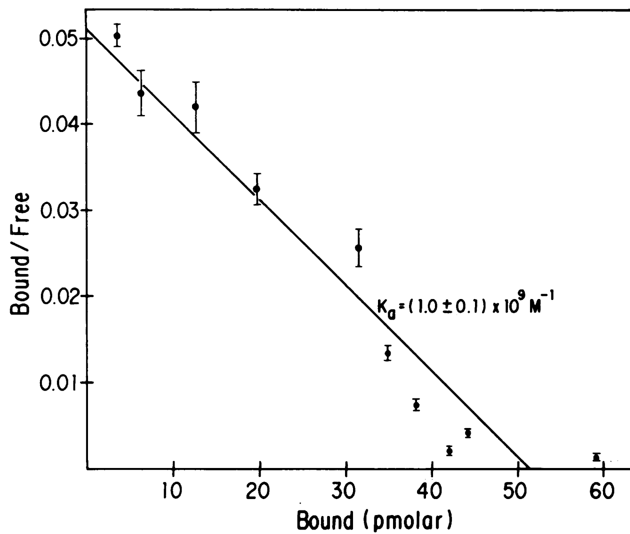

FIG. 1. Determination of the affinity constant (K_a) of Mel-14 F(ab')$_2$ after labeling with ^{211}At. ^{211}At-labeled Mel-14 F(ab')$_2$ was incubated with antigen-positive TE-671 human medulloblastoma cells and, to correct for nonspecific binding, antigen-negative human fibroblasts.

Tumor/normal tissue ratios of ^{211}At after injection of ^{211}At-labeled Mel-14 F(ab')$_2$ and control RPC 5 F(ab')$_2$ are compared in Fig. 3. Higher tumor/tissue ratios were obtained with Mel-14 F(ab')$_2$ at all time points. Tumor/blood ratios for ^{211}At-labeled Mel-14 F(ab')$_2$ increased from 0.7 ± 0.1 at 3 hr to 5.8 ± 0.4 at 24 hr, while tumor/blood ratios for RPC 5 F(ab')$_2$ were 0.4 ± 0.1 at 3 and 24 hr. At 24 hr, tumor/tissue ratios of Mel-14 F(ab')$_2$ ranged from 8-fold (muscle) to 15-fold (blood) higher than those obtained with RPC 5 F(ab')$_2$.

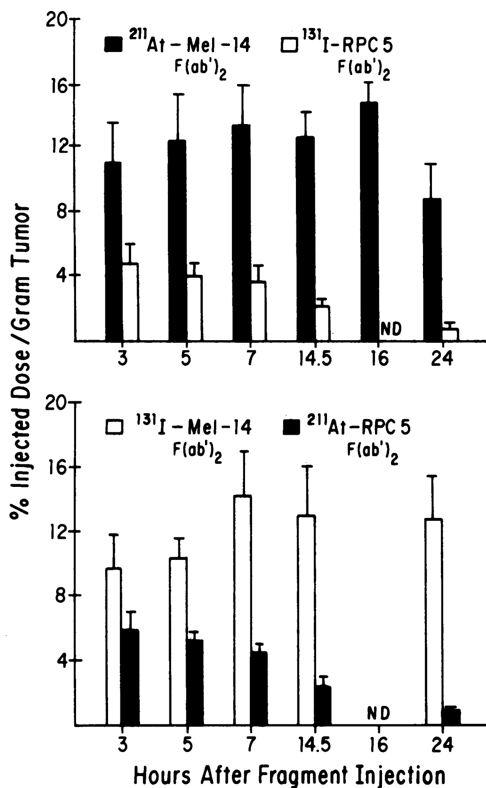

FIG. 2. Localization of labeled F(ab')$_2$ fragments in D-54 MG subcutaneous human glioma xenografts implanted in athymic mice. Each experimental value is expressed as the mean percent injected dose per gram of tumor ± standard deviation for 5–6 animals. ND, not determined.

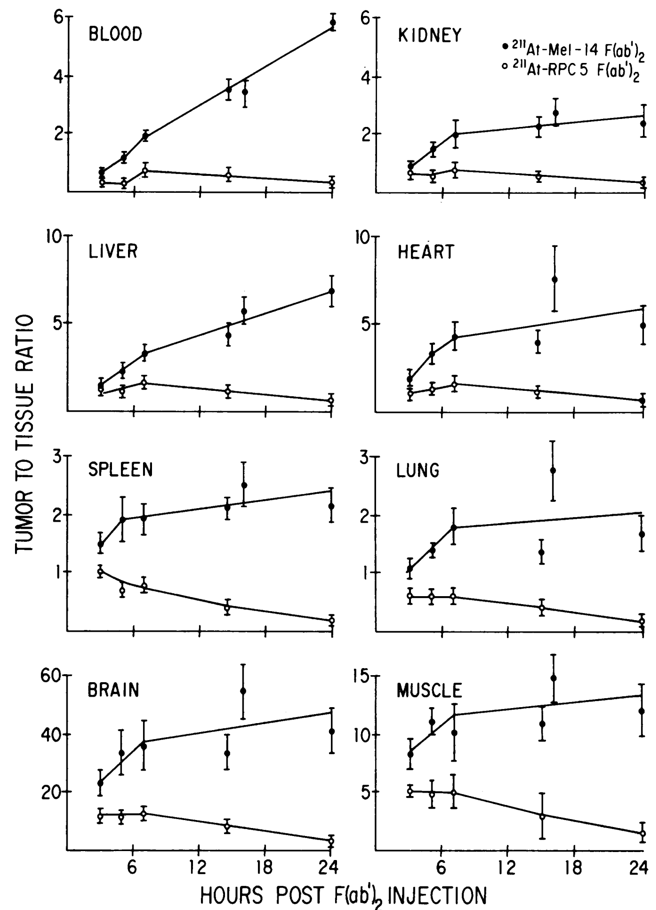

FIG. 3. Tumor/normal-tissue uptake ratios in athymic mice bearing D-54 MG subcutaneous human glioma xenografts. ●, ^{211}At-labeled Mel-14 F(ab')$_2$; ○, ^{211}At-labeled nonspecific RPC 5 F(ab')$_2$. Values are the mean ± standard deviation for 5–6 animals.

Localization indices for ^{211}At-labeled Mel-14 F(ab')$_2$, normalized to tissue uptake values for ^{211}At-labeled RPC 5 F(ab')$_2$, are summarized in Table 1. In subcutaneous tumors, the localization index increased from 1.7 ± 0.3 at 3 hr to 12.4 ± 0.4 at 24 hr, reflecting the specificity of tumor uptake of ^{211}At-labeled Mel-14 F(ab')$_2$. In contrast, localization indices in normal tissues indicated similar distribution of ^{211}At-labeled specific and control F(ab')$_2$. When normalized to coinjected ^{131}I-labeled RPC 5 F(ab')$_2$, localization indices for ^{211}At-labeled Mel-14 F(ab')$_2$ in tumor increased from 2.6 ± 0.1 at 3 hr to 11 ± 1 at 24 hr.

Tissue distribution data were used to calculate radiation absorbed doses per 100 μCi of ^{211}At-labeled specific and control F(ab')$_2$ (Table 2). An estimated 1920 rads was delivered to these tumors by ^{211}At-labeled Mel-14 F(ab')$_2$, a value almost 5-fold greater than that delivered by RPC 5 F(ab')$_2$. Radiation doses to normal tissues for Mel-14 F(ab')$_2$ ranged from 53 rads for brain to 1147 rads for lungs. Normal tissue doses for RPC 5 F(ab')$_2$ were quite similar.

DISCUSSION

In this study, we have demonstrated that intact mAbs and F(ab')$_2$ fragments can be labeled with ^{211}At in high yield in a time frame compatible with the 7.2-hr half-life of this nuclide. NS[^{211}At]AB was synthesized at a no-carrier-added level from a trimethylstannyl precursor (*m*-MeATE). The asta-

Downloaded at Palestinian Territory, occupied on November 28, 2021

Table 1. Localization indices following the injection of ^{211}At-labeled Mel-14 F(ab′)$_2$ and RPC 5 F(ab′)$_2$ fragments

Tissue	Localization index*				
	3 hr	5 hr	7 hr	14.5 hr	24 hr
Tumor	1.7 ± 0.3	2.9 ± 0.4	3.1 ± 0.3	5.9 ± 1.4	12.4 ± 0.4
Liver	1.4 ± 0.3	1.5 ± 0.5	1.6 ± 0.5	1.7 ± 0.7	1.4 ± 0.5
Spleen	1.1 ± 0.3	1.2 ± 0.3	1.4 ± 0.4	1.3 ± 0.5	1.4 ± 0.4
Lung	1.0 ± 0.2	1.2 ± 0.3	1.1 ± 0.2	1.6 ± 0.7	1.4 ± 0.6
Kidney	1.2 ± 0.3	1.3 ± 0.3	1.4 ± 0.3	1.6 ± 0.5	1.7 ± 0.6
Stomach	1.2 ± 0.4	1.7 ± 0.8	1.3 ± 0.5	1.2 ± 0.5	1.0 ± 0.6
Thyroid	1.1 ± 0.3	1.7 ± 0.4	1.1 ± 0.4	1.3 ± 0.5	1.2 ± 0.6
Muscle	1.1 ± 0.2	1.4 ± 0.3	1.5 ± 0.6	1.6 ± 0.6	1.8 ± 0.8
Blood	1	1	1	1	1

*The ratio of ^{211}At-labeled Mel-14 F(ab′)$_2$ to ^{211}At-labeled RPC 5 F(ab′)$_2$ in tissue divided by the same ratio in blood. Values are mean ± standard deviation with 5–6 animals per time point for each mAb fragment.

todestannylation of tri-*n*-butylstannyl compounds in the absence of iodide carrier has been reported previously (15, 24).

The procedure described herein incorporates several significant modifications of our initial method for labeling proteins with ^{211}At by means of *m*-BuATE. Increasing the distillation temperature resulted in a 2- to 3-fold decrease in the time required for isolation of ^{211}At from the cyclotron target. When necessary, the apparatus between the furnace and the trap could be rinsed with $CHCl_3$ to yield an additional 10–20% of ^{211}At activity. In organic solvents such as $CHCl_3$, ^{211}At is most likely present as AtX, where X is either a halogen or an organic impurity (25, 26). Reaction with *m*-MeATE and *t*-butyl hydroperoxide resulted in almost quantitative yield of NS[^{211}At]AB. Previously, ^{211}At was isolated in dilute sodium hydroxide, presumably as $At(OH)_2^-$ (27). Under these conditions, about one-third of the ^{211}At was associated with a by-product considered to be a π complex between AtX and the ATE aromatic ring (15). Minimizing the aqueous content of the astatination reaction mixture also is advantageous because it should decrease the hydrolysis of NS[^{211}At]AB, resulting in higher protein coupling efficiencies.

An additional modification was the substitution of *m*-MeATE for the *m*-BuATE precursor used previously (15). Decreasing the bulk of the alkyltin substituent has been shown to increase the rate of iododestannylation (17, 28); because of the greater size of the astatine atom, use of the trimethyltin derivative should be advantageous. Although a detailed kinetic study was not performed, higher yields of NS[^{211}At]AB consistently were obtained for the astatodestannylation of *m*-MeATE. Finally, HPLC purification of NS[^{211}At]AB increased mAb labeling efficiencies, probably by minimizing the interference of the lipophilic *m*-MeATE precursor in the protein coupling reaction.

Table 2. Radiation absorbed dose per 100 μCi of ^{211}At-labeled Mel-14 F(ab′)$_2$ or RPC 5 F(ab′)$_2$ fragment administered to mice bearing subcutaneous D-54 MG tumors

Tissue	Absorbed dose, rads (cGy)	
	^{211}At-Mel-14 F(ab′)$_2$	^{211}At-RPC 5 F(ab′)$_2$
Tumor	1920	422
Brain	53	56
Liver	595	494
Kidney	1108	1029
Spleen	826	854
Heart	524	530
Lung	1143	1245
Muscle	142	137
Blood	1083	1346

Although the astatination of mAbs has been reported (29–31), retention of immunocompetence after ^{211}At labeling was not demonstrated. In the present study, we have shown that 81C6 IgG2b mAb and Mel-14 IgG2a F(ab′)$_2$ fragment can be labeled with ^{211}At and retain their specific binding to human glioma homogenates *in vitro*. Indeed, the specific binding percentages observed were greater than those reported previously for the same mAbs radioiodinated by the Iodogen method (19, 32) and were comparable to the percentages for these mAbs after radioiodination using ATE (17, 33). The higher immunoreactivity of mAbs labeled by the ATE method could reflect the fact that this approach avoids exposure of mAbs to potentially denaturing oxidants such as those used in electrophilic iodinations.

Previous studies *in vivo* with ^{211}At-labeled mAbs have not shown preferential uptake of ^{211}At in tumor (29, 30, 34), suggesting that the labeled mAbs were of low immunoreactivity or were deastatinated *in vivo*. In this study, ^{211}At-labeled Mel-14 F(ab′)$_2$ was shown to localize preferentially in human glioma xenografts in athymic mice. The biokinetics of the astatinated mAb fragment appear to be well suited to the 7.2-hr half-life of ^{211}At, since tumor uptake remained high for >2 half-lives after injection and decreased only slightly at 24 hr. Except at 24 hr, tumor localizations of ^{211}At-labeled and ^{131}I-labeled Mel-14 F(ab′)$_2$ were quite similar. Indeed, the tumor uptake of ^{211}At-labeled Mel-14 F(ab′)$_2$ was higher than that of Mel-14 F(ab′)$_2$ radioiodinated by a conventional method (14).

A standard paired-label format could not be performed to evaluate specificity because of the lack of a suitable astatine nuclide for coadministration with ^{211}At. Localization indices were calculated by normalizing both to coinjected RPC 5 F(ab′)$_2$ labeled with ^{131}I by the ATE method and to ^{211}At-labeled RPC 5 F(ab′)$_2$ injected in a second group of animals. In both comparisons, ^{211}At-labeled Mel-14 F(ab′)$_2$ exhibited specific localization in tumor at all time points.

Because of the short pathlength of α-particles in tissue, the dose to different regions in both normal tissues and tumor could vary over a wide range. Accurate calculation of ^{211}At radiation dosimetry requires data concerning its microscopic distribution in tissue and the use of a microdosimetric model that accounts for the stochastic variation of α-particle hits and energy deposition at a subcellular level (35). However, in order to provide an initial estimate of the radiation dosimetry of ^{211}At-labeled mAbs, uniform distribution of activity in tissue was assumed. From the biodistribution data obtained in this study, a radiation dose of >1900 rads was predicted for a 100-μCi dose of ^{211}At-labeled Mel-14 F(ab′)$_2$, a value almost 5-fold greater than that of nonspecific F(ab′)$_2$. The calculated dose to tumor from ^{211}At-labeled Mel-14 F(ab′)$_2$ is 2- to 15-fold higher per millicurie than those reported for

Downloaded at Palestinian Territory, occupied on November 28, 2021

^{131}I-labeled intact mAbs in mouse tumor xenografts (19, 32, 36–38) and 15 times the tumor dose reported previously for ^{131}I-labeled Mel-14 F(ab')$_2$ (14). Although tumor/normal-tissue dose ratios for ^{211}At- and ^{131}I-labeled Mel-14 F(ab')$_2$ fragments were comparable for blood, heart, and kidneys, higher doses to liver, lungs, and spleen were calculated for ^{211}At-labeled mAb, presumably reflecting the observation of a >10-fold higher retention of astatide, compared to iodide, in these tissues (39).

These studies were performed in a subcutaneous tumor model in order to demonstrate the selectivity and specificity of ^{211}At-labeled mAb uptake *in vivo*. It is envisioned, however, that the half-life and radiation properties of ^{211}At might be most effectively exploited in clinical settings favorable for compartmental delivery, such as intrathecal administration for leptomenningeal neoplastic disease and intraperitoneal administration for neoplastic ascites of ovarian carcinoma. Intracompartmental delivery has been shown to increase the rate of tumor uptake of labeled mAbs and decrease the dose to normal tissues (40, 41).

In summary, a method has been described for labeling mAbs and mAb F(ab')$_2$ fragments with the α-emitting nuclide ^{211}At in high yield and in a time frame compatible with its 7.2-hr half-life. mAbs and fragments have been labeled to a specific activity of 4 mCi/mg (about 1 astatine per 700 mAb molecules), a level at least 10-fold higher than reported previously (9, 10, 33–35) and greater than that calculated to be necessary for radioimmunotherapeutic studies in humans (42). After labeling with ^{211}At, the specific binding and affinity of an IgG2a F(ab')$_2$ fragment and an IgG2b immunoglobulin were retained. *In vivo* experiments suggest that selective and specific uptake of ^{211}At in human tumor xenografts can be achieved following administration of ^{211}At-labeled mAb F(ab')$_2$ fragments. Taken together, these data suggest that the feasibility of radioimmunotherapeutic strategies involving the use of ^{211}At-labeled mAbs and their fragments should be explored.

We thank Susan Slade and Cary Harrison for excellent technical assistance, John Need and Michael Dailey for performing the cyclotron irradiations, and Ann Tamariz for help in preparing the manuscript. This work was supported in part by National Cancer Institute Grants CA42324, CA11898, CA44640, and 5-P50-NS 20023 and by Grant CH403 from the American Cancer Society.

1. Barendsen, G. W., Koot, C. J., van Kersen, G. R., Bewley, D. K., Field, S. B. & Parnell, C. J. (1966) *Int. J. Radiat. Biol.* **10**, 317–327.
2. Bertsche, U., Iliakis, G. & Kraft, G. (1983) *Radiat. Res.* **95**, 57–67.
3. Ritter, M. A., Cleaver, J. E. & Tobias, C. A. (1977) *Nature (London)* **266**, 653–655.
4. Kozak, R. W., Atcher, R. W., Gansow, O. A., Friedman, A. M., Hines, J. J. & Waldmann, T. A. (1986) *Proc. Natl. Acad. Sci. USA* **83**, 474–478.
5. Macklis, R. M., Kinsey, B. M., Kassis, A. I., Ferrara, J. L. M., Atcher, R. W., Hines, J. J., Coleman, C. N., Adelstein, S. J. & Burakoff, S. J. (1988) *Science* **240**, 1024–1026.
6. Kassis, A. I., Harris, C. R., Adelstein, S. J., Ruth, T. J., Lambrecht, R. M. & Wolf, A. P. (1986) *Radiat. Res.* **105**, 27–36.
7. Aaij, C., Tschroots, W. R. J. M., Lindner, L. & Feltkamp, T. E. W. (1975) *Int. J. Appl. Radiat. Isot.* **26**, 25–30.
8. Vaughan, A. T. M. & Fremlin, J. H. (1978) *Int. J. Nucl. Med. Biol.* **5**, 229–230.
9. Friedman, A. M., Zalutsky, M. R., Wung, W., Buckingham, F., Harper, P. V., Jr., Scheer, G. H., Wainer, B., Hunter, R. L., Appelman, E. H., Rothberg, R. M., Fitch, F. W., Stuart, F. P. & Simonian, S. J. (1977) *Int. J. Nucl. Med. Biol.* **4**, 219–224.
10. Harrison, A. & Royle, L. (1984) *Int. J. Appl. Radiat. Isot.* **35**, 1005–1008.
11. Bourdon, M., Wilkstand, C. J., Furthmayr, H., Matthews, T. & Bigner, D. D. (1983) *Cancer Res.* **43**, 2796–2805.
12. Bourdon, M. A., Matthews, T. J., Pizzo, S. V. & Bigner, D. D. (1985) *J. Cell. Biochem.* **28**, 183–195.
13. Carrel, S., Accolla, R. S., Carmagnola, A. L. & Mach, J.-P. (1980) *Cancer Res.* **40**, 2523–2528.
14. Colapinto, E. V., Humphrey, P. A., Zalutsky, M. R., Groothuis, D. R., Friedman, H. S., de Tribolet, N., Carrel, S. & Bigner, D. D. (1988) *Cancer Res.* **48**, 5701–5707.
15. Zalutsky, M. R. & Narula, A. S. (1988) *Appl. Radiat. Isot.* **39**, 227–232.
16. Lambrecht, R. M. & Mirzadeh, S. (1985) *Appl. Radiat. Isot.* **36**, 443–450.
17. Garg, P. K., Archer, G. E., Jr., Bigner, D. D. & Zalutsky, M. R. (1989) *Appl. Radiat. Isot.* **40**, 485–490.
18. Zalutsky, M. R. & Narula, A. S. (1987) *Appl. Radiat. Isot.* **38**, 1051–1057.
19. Lee, Y.-S., Bullard, D. E., Zalutsky, M. R., Coleman, R. E., Friedman, H. S., Colapinto, E. V. & Bigner, D. D. (1988) *Cancer Res.* **48**, 559–566.
20. Friedman, H. S., Bigner, S. H., McComb, R. D., Schold, S. C., Pasternak, J. F., Groothuis, D. R. & Bigner, D. D. (1983) *J. Neuropathol. Exp. Neurol.* **42**, 485–503.
21. Singer, K. H., Scearce, R. M., Tuck, D. T., Whichard, L. P., Denning, S. M. & Haynes, B. F. (1989) *J. Invest. Dermatol.* **92**, 166–170.
22. McPherson, G. A. (1983) *Comput. Programs Biomed.* **17**, 107–113.
23. Moshakis, V., McIhinney, R. A., Raghaven, D. & Neville, A. M. (1981) *Br. J. Cancer* **44**, 91–99.
24. Pillai, K. M. R., McLaughlin, W. H., Lambrecht, R. M. & Bloomer, W. D. (1987) *J. Labelled Compd. Radiopharm.* **24**, 1117–1122.
25. Berei, K. (1985) *Gmelin Handbook of Inorganic Chemistry: Astatine* (Springer, Berlin), pp. 110–276.
26. Narula, A. S. & Zalutsky, M. R. (1989) *Radiochim. Acta*, in press.
27. Visser, G. W. M. & Diemer, E. L. (1983) *Radiochim. Acta* **33**, 145–151.
28. Wursthorn, K. R., Kuivila, H. G. & Smith, G. F. (1979) *J. Am. Chem. Soc.* **100**, 2779–2789.
29. Vaughan, A. T. M., Bateman, W. J. & Fisher, D. R. (1982) *Int. J. Radiat. Oncol. Biol. Phys.* **8**, 1943–1946.
30. Vaughan, A. T. M., Bateman, W. J., Brown, G. & Cowan, J. (1982) *Int. J. Nucl. Med. Biol.* **9**, 167–171.
31. Harrison, A. & Royle, L. (1987) *Natl. Cancer Inst. Monogr.* **3**, 157–158.
32. Lee, Y., Bullard, D. E., Humphrey, P. A., Colapinto, E. V., Friedman, H. S., Zalutsky, M. R., Coleman, R. E. & Bigner, D. D. (1988) *Cancer Res.* **48**, 2904–2910.
33. Garg, P. K., Slade, S., Harrison, C. & Zalutsky, M. R. (1989) *Nucl. Med. Biol.* **16**, in press.
34. Bateman, W. J., Vaughan, A. T. M. & Brown, G. (1983) *Int. J. Nucl. Med. Biol.* **10**, 241–244.
35. Humm, J. L. (1987) *Int. J. Radiat. Oncol. Biol. Phys.* **13**, 1767–1773.
36. Badger, C. C., Krohn, K. A., Peterson, A. V., Shulman, H. & Bernstein, I. D. (1985) *Cancer Res.* **45**, 1536–1544.
37. Sharkey, R. M., Pykett, M. J., Siegel, J. A., Alger, E. A., Primus, F. J. & Goldenberg, D. M. (1987) *Cancer Res.* **47**, 5672–5677.
38. Buchegger, F., Vacca, A., Carrel, S., Schreyer, M. & Mach, J.-P. (1988) *Int. J. Cancer* **41**, 127–134.
39. Hamilton, J. G., Asling, C. W., Garrison, W. M. & Scott, K. G. (1953) *Univ. Calif. Publ. Pharmacol.* **2**, 283–343.
40. Ward, B. G., Mather, S. J., Hawkins, L. R., Crowther, M. E., Shepard, J. H., Granowska, M., Britton, K. E. & Slevin, M. L. (1987) *Cancer Res.* **47**, 4719–4723.
41. Lashford, L. S., Davies, A. G., Richardson, R. B., Bourne, S. P., Bullmore, J. A., Eckhert, H., Kemshead, J. T. & Coakham, H. B. (1988) *Cancer* **61**, 857–868.
42. Bigler, R. E., Zanzonico, P. B. & Sgouros, G. (1988) *J. Nucl. Med.* **29**, 858 (abstr.).

Downloaded at Palestinian Territory, occupied on November 28, 2021